Available online at www.sciencedirect.com
SCIENCE DIRECT®
Dyes and Pigments 62 (2004) 11–19
DYES and PIGMENTS
www.elsevier.com/locate/dyepig

Reverse saturable absorption of copper phthalocyanines in toluene and sol-gel tetraethyl orthosilicate/polyvinyl butyral hybrid film

Andrew Teh Hu[a,*], Wei-Ya Wang[a], Jun Rong Chen[a], Lung-Chang Liu[a], Chia-Hon Tai[a], Tai-Huei Wei[b]

[a]*Department of Chemical Engineering, National Tsing-Hua University, Hsin-Chu, Taiwan, ROC*
[b]*Department of Physics, National Chung-Cheng University, Chia-Yi, Taiwan, ROC*

Received 23 July 2003; received in revised form 12 September 2003; accepted 20 October 2003

Abstract

Materials with strong reverse saturable absorption have been searched for power limiting applications, and metallophthalocyanine molecules are one of them. Here we report our investigations of reverse saturable absorptive properties of copper phthalocyanines with three different side substitutions. By dissolving them in toluene or incorporating them in polymer-silica hybrid material using a sol-gel process with polyvinyl butyral and tetraethyl orthosilicate as precursors, we found that substitution of copper phthalocyanines influence the optical nonlinearities. Regarding the preparation process of phthalocyanines in the solids, a new route has been successfully used.

Keywords: Reverse saturable absorption; Phthalocyanines; Sol-gel; Hybrid film

1. Introduction

Materials with strong reverse saturable absorption (RSA) can effectively limit the output energy of incident light. Such materials are of prime importance in optical limiting applications [1]. Metallophthalocyanine (MPc) molecules have become widely-researched because their planar π-conjugated electron systems are expected to cause strong RSA effect [2,3]. Recently, organic-inorganic hybrid materials have attracted much attention for their flexibility, high glass transition temperature, good transparency, and potential as device substrates.

In this paper, we quantitatively characterized RSA of copper phthalocyanines (CuPc) with three different substitutions (α-tetra-cumylphenoxyl, β-tetra-cumylphenoxyl, and β-tetra-*tert*-butyl, dubbed as $(\alpha\text{-CP})_4$, $(\beta\text{-CP})_4$, and $(\beta\text{-}t\text{-butyl})_4$ respectively) in toluene solution and in sol-gel tetraethyl orthosilicate (TEOS)/polyvinyl butyral (PVB) hybrid film by using *Z*-scan technique with picosecond (ps) laser pulses at 532 nm. As a result, we found that CuPc $(\beta\text{-}t\text{-butyl})_4$ shows the strongest RSA when dissolved in toluene solution; however, CuPc $(\alpha\text{-CP})_4$ reveals the strongest RSA when incorporated in thin films.

* Corresponding author. Tel.: +886-3-571-3830; fax: +886-3-571-5408.
E-mail address: athu@che.nthu.edu.tw (A. T. Hu).

0143-7208/$ - see front matter © 2003 Elsevier Ltd. All rights reserved.
doi:10.1016/j.dyepig.2003.10.018

2. Experimental

2.1. Preparation of dyes and organic-inorganic hybrid films

CuPc (α-CP)$_4$, CuPc (β-CP)$_4$ and CuPc (β-*t*-butyl)$_4$ were prepared from phthalonitriles and copper chlorides by the procedure reported previously [5,6] and purified by silicon column chromatography. The chemical structures of CuPc (α-CP)$_4$, CuPc (β-CP)$_4$ and CuPc (β-*t*-butyl)$_4$ are shown in Fig. 1.

Sol A was prepared by mixing TEOS, H_2O, ethanol, and 1 N $HCl_{(aq.)}$ (1:8:3:10^{-4} = mole ratio) together. The mixture was stirred at room temperature for 12 h to obtain a homogeneous solution. Sol B was prepared by dissolving dyes (0.1 wt.%) and polyvinyl butyral (PVB) in propylene glycol methyl ether acetate. Then Sol A and Sol B were mixed and stirred at 60 °C for 12 h. By casting the gel, the hybrid films were made. The films were dried slowly in air at room temperature for one day, then the gels were vacuum-dried at 50 °C for 3 h and 130 °C for 2 h, respectively. Finally, blue and transparent dried films, whose thickness were approximately 100 μm, were obtained. The chemical structure of TEOS/PVB matrix is shown in Fig. 2.

2.2. Z-scan measurements

Comparative *Z*-scan experiments were executed on the toluene solutions and hybrid films of CuPc (α-CP)$_4$, CuPc (β-CP)$_4$, and CuPc (β-*t*-butyl)$_4$, respectively. This technique has been introduced previously [7]. Briefly it hinges on intensity (energy per area per time and denoted by I henceforth) attenuation of a Gaussian laser beam after nonlinearly interacting with the samples located at various positions along the beam propagation direction (z).We recorded the transmittance (transmitted energy divided by the input energy) as a function of z. Figs. 3–7 shows the recording transmittance vs. z curves after normalized to yield a unity transmittance in the linear regions. These curves, referred to as the *Z*-scan curves, all reveal a transmittance minimum at z = 0. While the input energy is fixed at each z position, this feature reveals transmittance decreases as I or fluence (defined as time integral of intensity and denoted by F henceforth) increase. When transmittance variation is attributed to absorption change alone, the results further indicates the absorption coefficient α increases with I or F. This can be explained with the Beer's law equation

$$\frac{dI}{dz'} = -\alpha I \tag{1}$$

where z' is the penetration of the light into the sample. According to Ref. [7], when α increases with I or F, a material's absorption is referred to as RSA, in comparison with saturable absorption (SA) when α decreases as I or F increases and linear absorption when α maintains unchanged as I increases or F. In the following we will explain, for our samples, how α increases with I or F using the five state model.

In the linear regime, i.e., the regions of large $|z|$, the input intensity I_0 is very low and α is nearly a constant (α_0). Under this condition, we can integrate Eq. (1) and obtain the transmittance

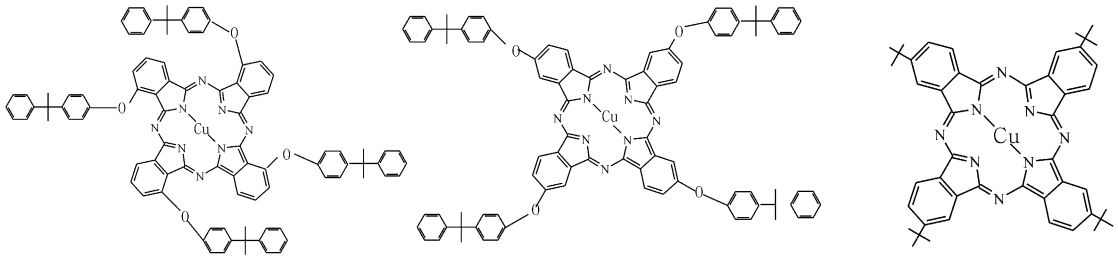

Fig. 1. The chemical structures of CuPc (α-CP)$_4$, CuPc (β-CP)$_4$ and CuPc (β-*t*-butyl)$_4$.

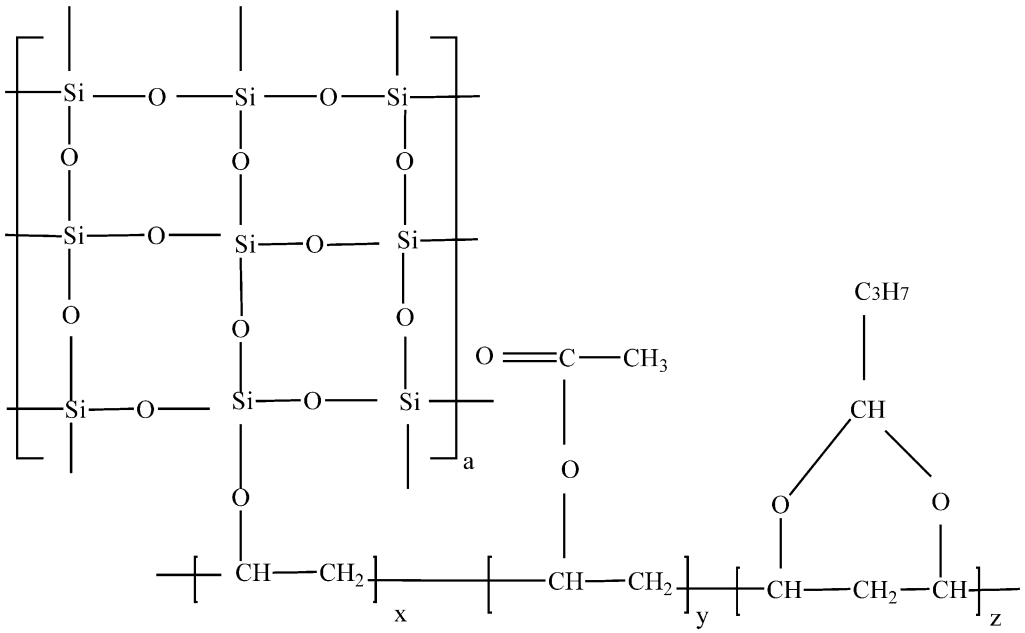

Fig. 2. The chemical structure of TEOS/PVB matrix.

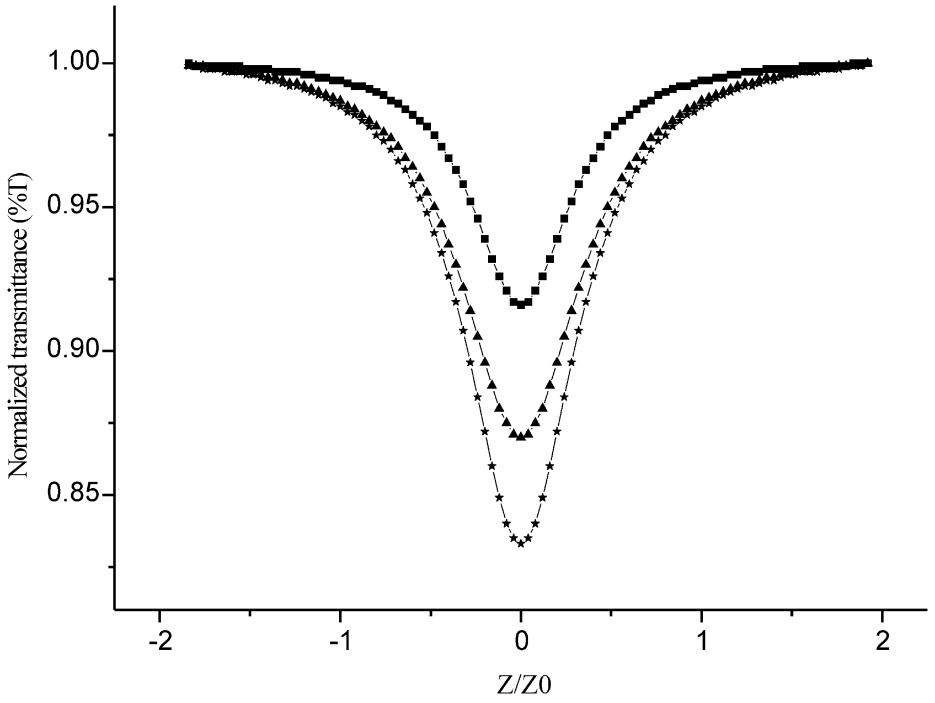

Fig. 3. Open aperture *Z*-scan results of CuPc solution at laser intensity of 1 μJ, rectangle represents CuPc (α-CP)$_4$, triangle represents CuPc (β-CP)$_4$ and star represents CuPc (β-*t*-butyl)$_4$, in each curve, and solid line for theoretical fits.

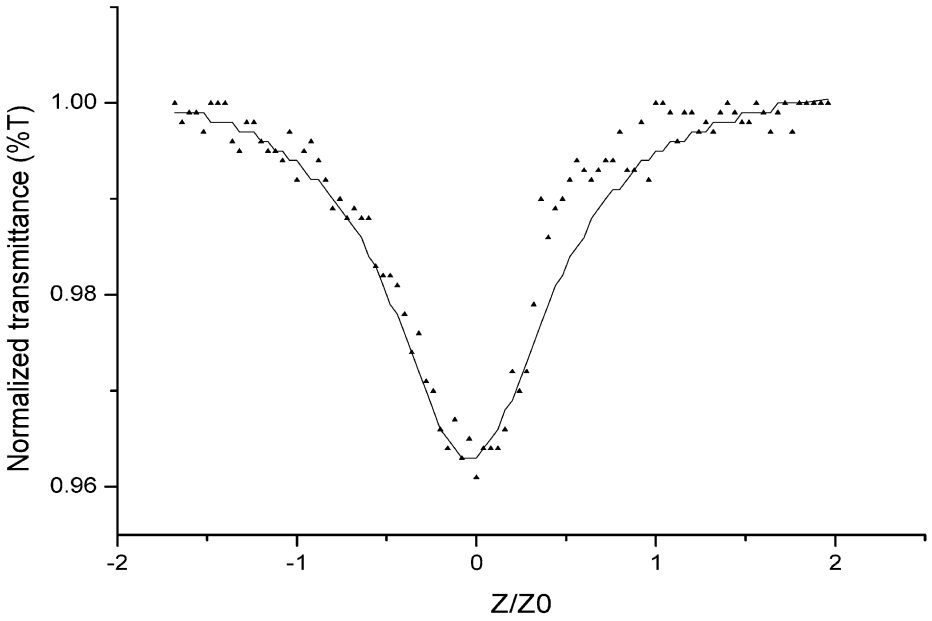

Fig. 4. Open aperture *Z*-scan results of CuPc $(\alpha\text{-CP})_4$ in hybrid film of input intensity of 1 μJ, triangle represents experimental data, and solid line for theoretical fits.

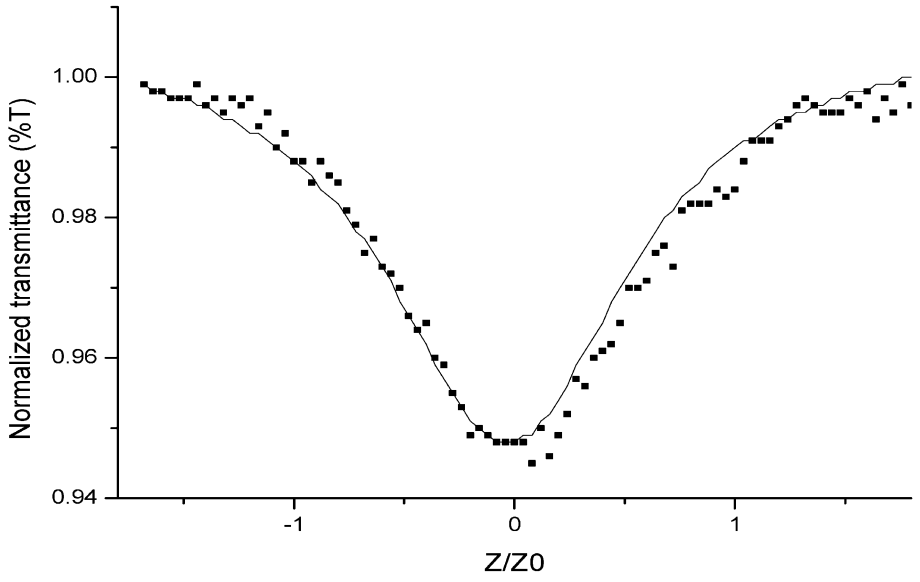

Fig. 5. Open aperture *Z*-scan results of CuPc $(\beta\text{-CP})_4$ in hybrid film of laser intensity of 1 μJ, where rectangle represents experimental data, and solid line for theoretical fits.

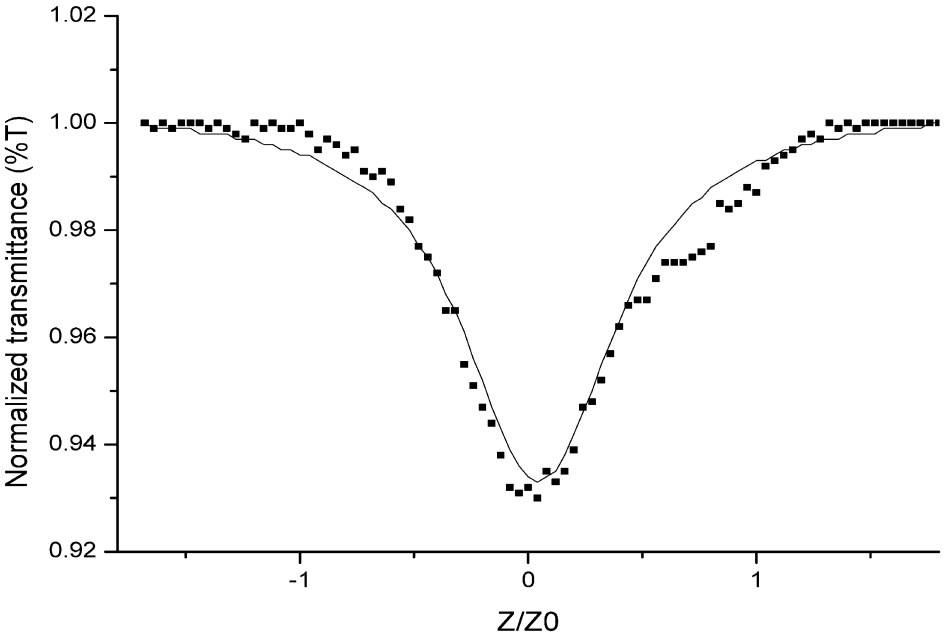

Fig. 6. Open aperture *Z*-scan results of CuPc (β-*t*-butyl)$_4$ in hybrid film of laser intensity of 1 μJ, where rectangle represents experimental data, and solid line for theoretical fits.

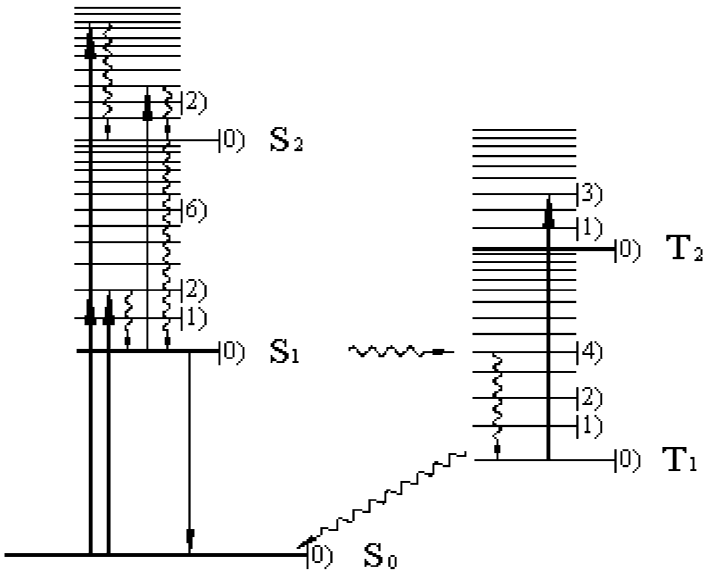

Fig. 7. The five-energy-level diagram showing optical excitation (upward-pointing arrows), nonradiative relaxation (wiggly lines), and radiative relaxation (downward-pointing arrows. $|\nu\rangle$ refers to the vibrational eigenstates involved in the transitions.

$$T \equiv \frac{I_l}{I_0} = e^{-\alpha_0 l} \tag{2}$$

where I_l represents the intensity at the rear surface of the sample and l denotes the sample thickness. Since $\log(1/T)$, referred to as absorption (A), is found to be proportional to the product of concentration C and l, i.e.,

$$A \equiv \log \frac{1}{T} = \varepsilon C l \tag{3}$$

we have $\alpha_0 = 2.303\varepsilon C$. In Eq. (3) ε is the proportional constant (extinction coefficient).

Optical excitation of our samples can be described using the five-energy-state scheme [8]. As shown in Fig. 5, each band, including the associated zero-point level $|0)$ and vibronic level $|\nu \neq 0)$, is named as S_m for the singlet manifold and T_m for the triplet manifold where subscript m refers to the state formed from certain electronic configurations in molecular orbitals. At thermal equilibrium, all the molecules π free electrons reside on the ground state $[S_0(\pi)]$. Pumped by 532 nm laser pulses, some of them are excited to $|\nu)S_1$ by one-photon absorption or to $|\nu)S_2$ via two-photon absorption. Those promoted to $\kappa\nu)S_1$ first relax to the zero point level $|0)$ and then undergo one of the following process: (i) decay to ground state radiatively (fluorescence) or nonradiatively (internal conversion), (ii) intersystem crossing (with a time constant and denoted by τ_{isc} henceforth), and (iii) one-photon excitation to S_2. Since in our investigation, the pulse duration is much shorter than τ_{isc}, the electron excitation to triplet state can be ignored, and the Beer's law equation can be written as

$$\frac{dI}{dz'} = -\alpha I = -[\sigma_{S0}N_{S0} + \sigma_{S1}N_{S1}]I - \beta N_{S0} I^2 \tag{4}$$

to express the mechanism of absorption in the ps regime. In Eq. (4), σ and N respectively represent the absorption cross-section and molecular concentration of the states specified by the footnotes.

Associated with Eq. (4), The population change rates are

$$\frac{dN_{S0}}{dt} = -\frac{\sigma_{S0}N_{S0}I}{h\omega} - \frac{\beta N_{S0} I}{2h\omega} \tag{5}$$

and

$$\frac{dN_{S1}}{dt} = \frac{\sigma_{S0}N_{S0}I}{h\omega} + \frac{\beta N_{S0} I^2}{2h\omega} - \frac{\sigma_{S1}N_{S1}I}{h\omega} + \frac{N_{S2}}{\tau_{S2}} \tag{6}$$

and

$$\frac{dN_{S2}}{dt} = \frac{\sigma_{S1}N_{S1}I}{h\omega} - \frac{N_{S2}}{\tau_{S2}} \tag{7}$$

where h represents the Planck constant divided by 2π and ω is the frequency of laser. At very low input intensity, α approaches α_0 and equals $\sigma_{S0}N_{S0}(-\infty)$.

As explained in Ref. [4], when $\sigma_{S1} > \sigma_{S0}$, α increases as F increases and thus the sample show RSA, when $\sigma_{S1} < \sigma_{S0}$, α decreases F increases and thus the sample show SA, and when $\sigma_{S1} = \sigma_{S0}$, the sample shows linear absorption with $\alpha = \alpha_0$.

In this study, a Q-switched and mode-locked Nd:YAG laser operated in the TEM_{00} mode at 10 Hz was used. The laser is frequency-doubled to give an output wavelength ($\lambda = 532$ nm) and tightly focused to have a radius of

$$\omega_0 = 28\ \mu m$$

at e^{-2} of maximum intensity at the focus. The pulse has a half-width of $\tau = 16.3$ ps at e^{-1} of maximum intensity (HW e^{-1} M).

In our investigation, all the solution samples are prepared to have a concentration of 10^{-4} M and contained in a 1 mm quartz cell. The hybrid films are made to have thickness ranging between 80 and 100 μm and have 0.1 wt.%. The films doped with dyes were put on the side of quartz vessel, and the laser can penetrate through them.

3. Results and discussion

3.1. Linear spectroscopy

On account of $S_0 \rightarrow S_1$ and $S_0 \rightarrow S_2$ transitions, phthalocyanines usually exhibit two characteristic absorptions [9,10], which are B band (300–400 nm) and Q band (600–800 nm), respectively. For phthalocyanine molecules, the interesting region of optical limiting effect lies in the highly transparent regime between 450 nm and

550 nm. Here we focused the region near 532 nm for instrumental consideration. The linear absorption spectra of CuPc (α-CP)$_4$), CuPc (β-CP)$_4$, and CuPc (β-*t*-butyl)$_4$ in toluene and hybrid film are shown in Figs. 8–10, respectively. Difference in the absorption band is due to aggregation taken place in hybrid film. Aggregation is the result of strong intermolecular interaction between the dyes and the matrix, which leads to blue shift and the broadness of band shape.

3.2. *Picosecond* Z*-scan measurements*

Using Eqs. (4)–(7), we numerically fit the *Z*-scan results (as shown in Figs. 3–7). The best fit (solid line in the figures) are obtained with the values of σ_{S1} shown in Table 1. σ_{S0} is derived from α_0 based on Eq. (3) while α_0 is measured in the linear region of the *Z*-scan apparatus. In Table 1, we also summarize σ_{S1}/σ_{S0} (a parameter to evaluate the limiting performance). Experimental results reveal that the σ_{S1}/σ_{S0} values of copper phthalocyanines in hybrid film are lower than those in toluene. It is postulated that the result of aggregation taken place in hybrid film doped with copper phthalocyanines. Aggregation causes intermolecular excition coupling leading to lowering of the excited state cross-section in the hybrid film.

In toluene, CuPc (β-*t*-butyl)$_4$ exhibits the best optical-limiting effect among these dyes. But in hybrid film, CuPc (α-CP)$_4$ exhibits highest σ_{s1}/σ_{s0} value than CuPc (β-*t*-butyl)$_4$ and CuPc (β-CP)$_4$, we surmise that the α-substitution with CuPc (α-CP)$_4$ has more serious steric hindrance and prevents the phthalocyanines ring from forming co-facial dimmers or high-order aggregates.

Table 1

Compound	σ_{so} (cm^2)		σ_{s1} (cm^2)		σ_{s1}/σ_{so}	
	Solution	Film	Solution	Film	Solution	Film
CuPc (α-CP)$_4$	4.0×10^{-18}	2.9×10^{-18}	6.9×10^{-17}	4.8×10^{-17}	17.3	3.9
CuPc (β-CP)$_4$	5.3×10^{-18}	7.6×10^{-18}	11.7×10^{-17}	2.3×10^{-17}	22.2	3.0
CuPc (β-t-but)$_4$	4.8×10^{-18}	1.2×10^{-17}	14.1×10^{-17}	3.1×10^{-17}	29.4	2.5

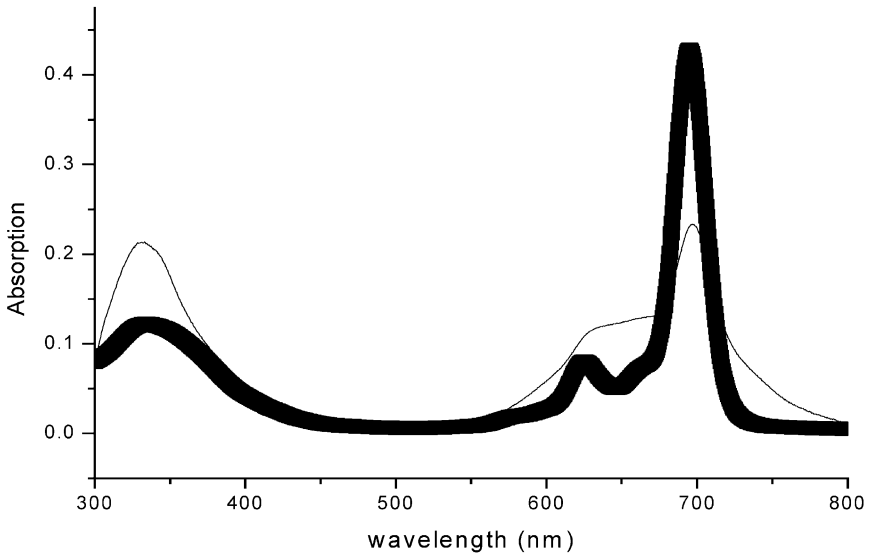

Fig. 8. UV–Vis spectra of CuPc (α-CP)$_4$ in toluene and film: the thick line represents solution and the thin line represents film.

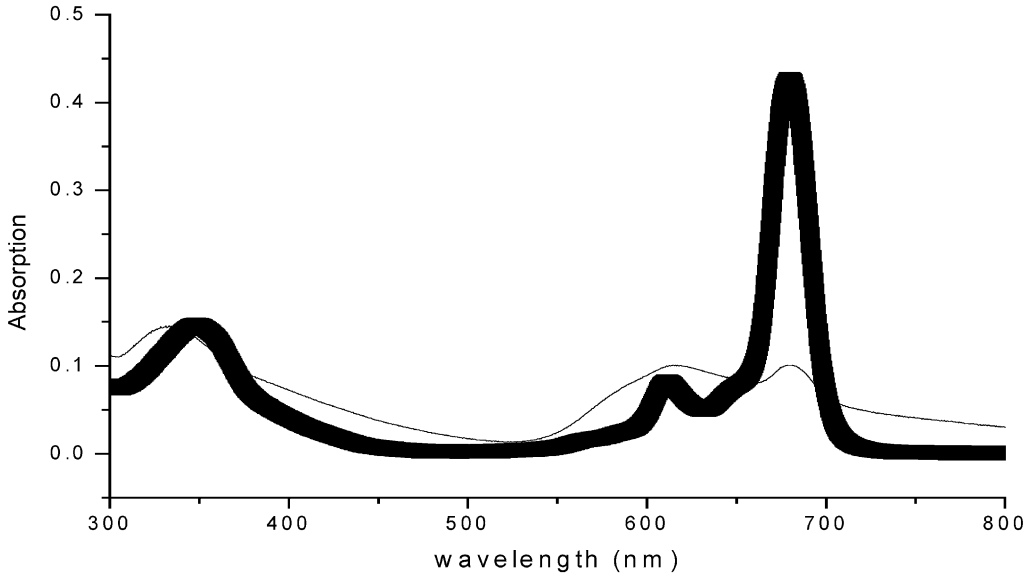

Fig. 9. UV-Vis spectra of CuPc (β-CP)$_4$ in toluene and film: the thick line represents solution and the thin line represents film.

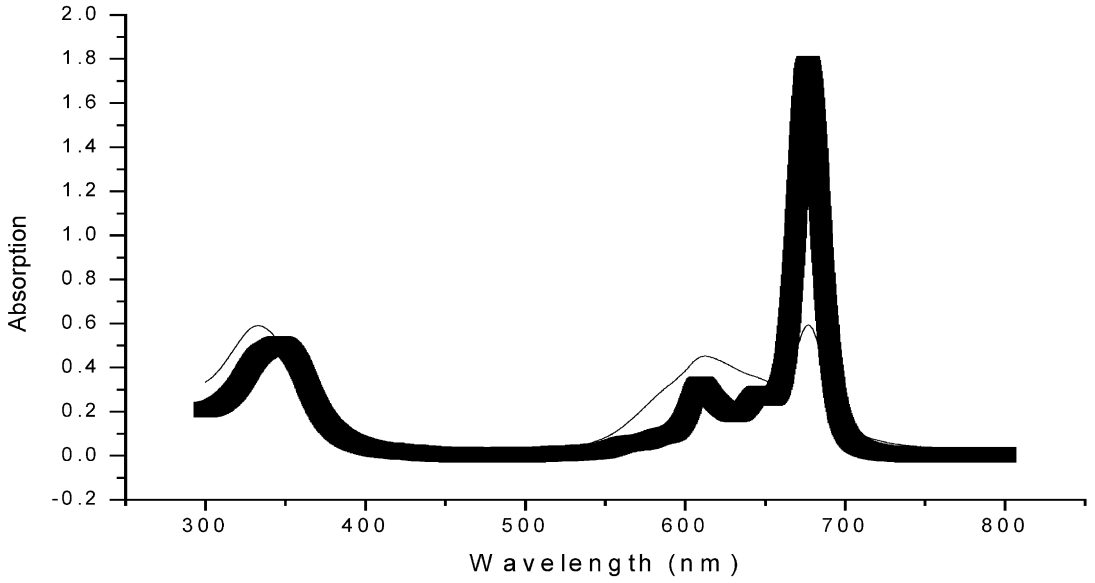

Fig. 10. UV–Vis spectra of CuPc (β-*t*-butyl)$_4$ in toluene and film: the thick line represents solution and the thin line represents film.

4. Conclusions

We have successfully prepared organic–inorganic hybrid films doped with copper phthalocyanines. The RSA properties in both solution and thin film have been investigated by *Z*-scan technique with picosecond laser pulse at 532 nm. In solution, CuPc (β-*t*-butyl)$_4$ exhibits the best RSA performance. But in hybrid films, RSA behavior of phthalocyanines are reduced due to aggregation. The hybrid film doped with CuPc (α-CP)$_4$, exhibits the strongest RSA properties because its

large steric hindrance property hampers its ability to aggregate.

Acknowledgements

We gratefully appreciate the financial support by National Science Council of Taiwan for A.T. Hu (NSC-902216E007032) and also thank professor T.H. Wei, National Chung-Cheng University, for instrumental support.

References

[1] (a) Iwase A, Harnoode C, Kameda Y. Journal of Alloys and Compounds 1993;192:280.
(b) Nalwa HS, Miyata S. Handbook of organic conductive molecules and polymers. Boca Raton: CRC Press; 1997.
[2] Leznoff CC, Lever ABP. Phthalocyanines. Properties and applications. Cambridge: VCH; 1996.
[3] Perry JW, Mansour K, Lee IYS, Wu XL, Bedworth PV, Chen CT, et al. Science 1996;273:1533.
[4] Bentivegna F, Canva M, Georges P, Brun A, Chaput F, Malier L, Boilot JP. Appl Phys Lett 1993;62:1271.
[5] Mikhalenko SA, Barknova SV, Lebedev OL, Luk'yanets EA. Zhurnal Obshchei Khimii 1971;41:2735.
[6] Shirk JW, Pong RGS, Flom SR, Bartoli FJ, Boyle ME, Snow AW. US patent, 805326, 1998.
[7] Wei TH, Huang TH, Wen TC. Chem Phys Lett 1999; 314:403.
[8] Wei TH, Huang TH. Optical and Quantum Electronics 1996;28:1495.
[9] McKeown NB. Phthalocyanine material synthesis, structure and function. Cambridge: Cambridge University Press; 1998.
[10] Leznoff CC, Lever ABP. Phthalocyanines properties and applications. Cambridge: VCH; 1989.